
Pragmatic Curiosity: A Hybrid Learning-Optimization Paradigm via Active Inference

Yingke Li¹ Anjali Parashar¹ Enlu Zhou² Chuchu Fan¹

Abstract

Many engineering and scientific workflows depend on expensive black-box evaluations, requiring decision-making that simultaneously improves performance and reduces uncertainty. Bayesian optimization (BO) and Bayesian experimental design (BED) offer powerful yet largely separate treatments of goal-seeking and information-seeking, providing limited guidance for hybrid settings where learning and optimization are intrinsically coupled. We propose *pragmatic curiosity*, a hybrid learning-optimization paradigm derived from *active inference*, in which actions are selected by minimizing the *expected free energy*—a single objective that couples pragmatic utility with epistemic information gain. We demonstrate the practical effectiveness and flexibility of pragmatic curiosity on various real-world hybrid tasks, including constrained system identification, targeted active search, and composite optimization with unknown preferences. Across these benchmarks, pragmatic curiosity consistently outperforms strong BO-type and BED-type baselines, delivering higher estimation accuracy, better critical-region coverage, and improved final solution quality.

1. Introduction

Engineering and scientific applications often rely on expensive black-box evaluations to identify high-performing designs or desirable system states. Bayesian optimization (BO) accelerates this process when the primary objective is to reach a specified *goal* (Shahriari et al., 2016; Frazier, 2018), whereas Bayesian experimental design (BED) prioritizes *information* acquisition about unknown system param-

¹Department of Aeronautics and Astronautics, Massachusetts Institute of Technology, Cambridge, MA 02139, USA ²School of Industrial and Systems Engineering, Georgia Institute of Technology, Atlanta, GA 30332, USA. Correspondence to: Chuchu Fan <chuchu@mit.edu>.

Preprint. February 9, 2026.

eters (Rainforth et al., 2023). Both methodologies leverage probabilistic models and acquisition criteria that quantify the utility of evaluating unknown configurations, tailored to either optimization or learning objectives. Despite their individual successes and the explosion of research in each field, their disconnection creates a vacuum for a broad class of hybrid problems that routinely require simultaneously both *seeking knowledge* and *achieving goals*.

For many real-world applications, such as goal-directed planning (Lookman et al., 2019), environmental monitoring (Konakovic Lukovic et al., 2020), and targeted material design (Matsumoto et al., 2025), *learning* and *optimization* are not separate phases but deeply intertwined objectives. This challenge fundamentally arises across tasks with increasing complexity in terms of both *epistemic consideration* (i.e., from parametric to non-parametric models) and *pragmatic evaluation* (i.e., from known to unknown goals):

(1) **Constrained System Identification**, where the *epistemic* desire of precisely learning a system’s parameters is governed by the *pragmatic* need to keep experiments within safe or valid operational bounds (e.g., avoiding sensor saturation, or dangerous chemical reaction). This type of task can be found in numerous applications, including environmental monitoring (Konakovic Lukovic et al., 2020) and catalyst design (Zhong et al., 2020).

(2) **Targeted Active Search**, where the *pragmatic* objective to discover regions that meet certain criteria (e.g., system failure modes, or specific performance ranges) requires *epistemic* curiosity to explore the region’s shape, size, and boundaries. Example applications can be found in failure discovery (Ramanagopal et al., 2018) and medical monitoring (Malkomes et al., 2021).

(3) **Composite Bayesian Optimization**, where the *pragmatic* goal is to find an optimal design based on a user’s hidden preferences—a task that is impossible without first being *epistemically* curious about the user’s objectives themselves. Such scenarios commonly arise in simulation-based design (González & Zavala, 2025; Coelho et al., 2025) and A/B testing (Bakshy et al., 2018).

Classically, to address these hybrid problems, practitioners have been forced to choose between specialized tools, and

accommodate problem-specific adaptation by leveraging information-gain criteria to enhance optimization and vice versa. On the BO side, Russo & Van Roy (2018) proposed information-directed sampling (IDS) to online optimization problems. Hvarfner et al. (2023) introduced a statistical distance-based active learning (SAL) criterion into the BO loop to actively learn the model hyperparameter even as it searches for the optimum. On the BED (also known as Bayesian active learning, BAL) side, Smith et al. (2023) proposed an expected predictive information gain (EPIG) criterion that focuses on information gain in model predictions, mitigating classical BAL’s tendency to select out-of-distribution or low-relevance queries by accounting for an input data distribution. These methods highlight growing synergy between optimization and learning, but they remain task-specific, and rarely generalize across categories.

In this paper, we propose **pragmatic curiosity**: a hybrid learning-optimization paradigm derived from *active inference* (AIF) (Friston, 2010; Friston et al., 2017). AIF prescribes action selection by minimizing *expected free energy* (EFE), a single objective that combines (i) a *pragmatic* term that favors preferred outcomes and (ii) an *epistemic* term that favors information gain. We prove that EFE minimization provides a unified perspective of various acquisition strategies: by specifying preferences, observation models, and approximations, the resulting criterion recovers BO-like and BED-like behaviors as limiting regimes.

Under this paradigm, seeking knowledge and achieving goals are not treated as competing objectives, but as two inseparable facets of a single imperative to minimize EFE. These two drives are balanced by a coefficient called *curiosity*, which sets the trade-off between learning and optimization. The formal role of curiosity in guaranteeing both *self-consistent learning* (i.e., posterior convergences to the truth) and *no-regret optimization* (i.e., with bounded cumulative regret) is provided *theoretically* in Li et al. (2026).

This paper, instead, demonstrates the **practical effectiveness and flexibility** of this paradigm in handling a broad class of complex hybrid problems often ignored by standard methods, including tasks with evolving goals (where conditions change over time) and implicit goals (where objectives are not defined *a priori*). We conduct experiments structured around the three problem classes mentioned above, drawing on applications that include environmental monitoring in plume fields (Konakovic Lukovic et al., 2020), failure detection in autonomous driving scenarios (Ramanagopal et al., 2018), and distributed energy resource allocation in power grids (Kianmehr et al., 2019).

The empirical results reveal a consistent pattern of superior performance, demonstrating our framework’s advantages in its ability to solve complex, hybrid objectives. In constrained system identification tasks, our algorithm achieved

near-perfect estimation accuracy while requiring up to 40% fewer queries than other methods. For targeted active search tasks, it demonstrated a more effective exploration strategy, discovering a crucial 10% more of the critical failure region within the same budget. Most notably, in tasks with unknown user preferences, our approach always successfully learned the underlying objective where other baselines fail to capture. Together, these findings validate the power of our unified approach, showing that a principled balance between pragmatic and epistemic drives leads to tangible gains across diverse and challenging problem settings.

In summary, our main contributions are the following:

- A **unified perspective** of various acquisition strategies through the lens of active inference.
- A **pragmatic curiosity paradigm** for general hybrid learning-optimization problems.
- A **comprehensive empirical validation** across three canonical real-world problem categories with diverse hybrid learning-optimization objectives.

2. Preliminaries

2.1. Bayesian Optimization

Given an unknown objective function $f : \mathcal{X} \mapsto \mathbb{R}$, BO seeks to identify the input x^* that maximizes the objective f over an admissible set of queries \mathcal{X} , i.e., $x^* = \arg \max_{x \in \mathcal{X}} f(x)$. To achieve this goal, BO relies on a *surrogate model* that provides a probabilistic representation of the objective f , and uses this information to compute an *acquisition function* to drive the selection of the most promising sample to query.

Surrogate model. We assume the available information regarding the objective function f be stored in the dataset $\mathcal{D}_t := \{(x_1, y_1), \dots, (x_t, y_t)\}$, where $y_t \sim \mathcal{N}(f(x_t), \sigma^2(x_t))$ is the noisy observation of the objective function by assuming the noise follows a zero-mean normal distribution with a standard deviation σ . The surrogate model depicts possible explanations of f as $f(x) \sim p(f(x)|\mathcal{D}_t)$ applying a joint distribution over its behavior at each sample $x \in \mathcal{X}$. In Bayesian inference, the prior distribution of the objective $p(f(x))$ is combined with the likelihood function $p(\mathcal{D}_t|f(x))$ to compute the posterior distribution $p(f(x)|\mathcal{D}_t) \propto p(\mathcal{D}_t|f(x))p(f(x))$, representing the updated beliefs about $f(x)$. Typically, Gaussian processes (GPs) have been widely used as the surrogate model for BO due to their efficient posterior sampling that enables cheap, gradient-based optimization of the acquisition function to propose new query points. GP is specified by a joint normal distribution $p(f(x)|\mathcal{D}_t) = \mathcal{N}(\mu_t(x), \kappa_t(x, x'))$ with mean $\mu_t(x)$ and kernel function $\kappa_t(x, x')$, where $\mu_t(x)$ represents

the prediction and $\kappa_t(x, x')$ the associated uncertainty.

Acquisition function. The surrogate model is utilized to decide the next sample $x_{t+1} \in \mathcal{X}$ through the maximization of an acquisition function $\alpha : \mathcal{X} \mapsto \mathbb{R}$, *i.e.*, $x_{t+1} = \arg \max_{x \in \mathcal{X}} \alpha(x | \mathcal{D}_t)$, where $\alpha(x | \mathcal{D}_t)$ provides a measure of the improvement that the next query is likely to provide with respect to (w.r.t.) the current surrogate model of the objective function. Many acquisition functions have been proposed, including *probability of improvement* (Močkus, 1975), *expected improvement* (Jones et al., 1998), *upper confidence bound*, and various *entropy search* methods (Hennig & Christian J. Schuler, 2012; Hernández-Lobato et al., 2014; Wang & Jegelka, 2017; Hvarfner et al., 2022a; Neiswanger et al., 2021), as well as practical approaches to optimize them (Wilson et al., 2018).

2.2. Bayesian Experimental Design

Rather than optimizing an objective function $f(x)$, the purpose of BED is to sequentially select a set of experimental designs $x \in \mathcal{X}$ and gather outcomes y , to maximize the amount of information obtained about certain *parameters of interest*, denoted as θ . The parameters θ can correspond to some explicit model parameters, or any implicitly defined quantity of interest (*e.g.*, the optimum of a function, the output of an algorithm, or future downstream predictions).

Based on the current history of experiments $\mathcal{D}_t := \{(x_1, y_1), \dots, (x_t, y_t)\}$, BED seeks to find the next experimental design x_{t+1} by maximizing the *expected information gain* (EIG) (Chaloner & Verdinelli, 1995) that a potential experimental outcome y_{t+1} can provide about θ , measured in terms of expected entropy reduction of the posterior distribution of θ :

$$\text{EIG}(x | \mathcal{D}_t) = H[p(\theta | \mathcal{D}_t)] - \mathbb{E}_{p(y|x, \mathcal{D}_t)}[H[p(\theta | \mathcal{D}_t \cup (x, y))]] \\ = I(\theta; (x, y) | \mathcal{D}_t),$$

where $H(\cdot)$ and $I(\cdot)$ denote the entropy and mutual information, respectively.

3. A Unified View of Acquisition Strategies

The acquisition strategies in BO typically lead to *goal-directed* behavior, where the (implicit) goal is the optimum of a certain (unknown) objective function. On the contrary, the acquisition strategies in BED encourage *information-seeking* behavior, aiming to gather the maximum amount of information about certain parameters of interest. Although they both can be viewed as realizations of adaptive sampling (Di Fiore et al., 2023), there are no transferable approaches between these two domains due to distinct directives (Hvarfner et al., 2025).

In this section, we show that these two seemingly competing imperatives can be naturally balanced through the principles

of active inference (AIF).

3.1. Active Inference as Expected Free Energy Minimization

We specify a probabilistic surrogate model $q(\cdot)$ to capture the relationship between an outcome y and a decision variable x based on a set of parameters s that are of interest, which factorizes as

$$q(x, y, s) := p(x, y | s)q(s),$$

where $q(x, y, s)$ is a joint probability distribution over (x, y, s) based on a surrogate distribution $q(s)$ over s . We use $q(\cdot)$ to explicitly distinguish this model to be an “surrogate” of the “true” model $p(\cdot)$.

One special aspect of AIF is the way it formalizes goals. Instead of specifying the goal with additional variables related to “rewards” or “costs”, AIF directly encodes the preferences over possible outcomes y through a probability distribution $p(y)$. In this distribution, outcomes with higher probabilities are treated as more rewarding. The deviation between observed outcomes and those desired is measured through an information-theoretic quantity known as *self-information* or *surprisal*: $-\log p(y)$. Intuitively, it’s a measure of how unexpected an outcome y is, given a prior preference distribution $p(y)$. Consistent with the intuitive notion of surprise, lower probability events generate higher surprisal values. Then the surprisal incurred from an observed outcome y is quantified by

$$\begin{aligned} -\log p(y) &= -\log \int p(y, s) ds \\ &= -\log \int \frac{p(y, s)q(s)}{q(s)} ds \\ &= -\log \mathbb{E}_{q(s)} \left[\frac{p(y, s)}{q(s)} \right] \\ &\leq -\mathbb{E}_{q(s)} \left[\log \frac{p(y, s)}{q(s)} \right] = F, \end{aligned} \tag{1}$$

where the last inequality follows *Jensen’s inequality*, which states that the expectation of a logarithm is always less than or equal to the logarithm of an expectation.

The right-hand side of (1) is called the *variational free energy* (VFE), whose name arises from the fact that F resembles the *Helmholtz free energy* in physics. We can see that VFE is always greater than or equal to surprisal (*i.e.*, it is an upper bound on surprisal). In machine learning, the sign of VFE is typically reversed, making it an *evidence lower bound* (ELBO). Maximizing the ELBO is a commonly used optimization approach in machine learning (Titsias, 2009).

To formulate a strategy for decision-making, we need to consider the decision variable x and the outcomes that result

from the choice of actions. Since the future outcomes have not yet occurred, we resort to examining the expectation of surprisal over predicted outcomes based on a predictive distribution $q(y|x)$:

$$\begin{aligned}
 & -\mathbb{E}_{q(y|x)} \log p(y|x) \\
 & \leq -\mathbb{E}_{q(y,s|x)} \left[\log \frac{p(y, s|x)}{q(s|x)} \right] \\
 & = -\mathbb{E}_{q(y,s|x)} \left[\log \frac{p(s|x, y)p(y|x)}{q(s|x)} \right] \\
 & = -\mathbb{E}_{q(y,s|x)} [\log p(s|x, y) - \log q(s|x)] \\
 & \quad - \mathbb{E}_{q(y,s|x)} \log p(y|x) \\
 & = -\mathbb{E}_{q(y,s|x)} [\log p(s|x, y) - \log q(s|x)] \\
 & \quad - \mathbb{E}_{q(y|x)} \log p(y|x) = G,
 \end{aligned} \tag{2}$$

where the right-hand side of (2) is denoted as the *expected free energy* (EFE).

Theorem 3.1. *When using a surrogate model $q(\cdot) = p(\cdot|\mathcal{D}_t)$ that is considered as the true model constructed from all available data \mathcal{D}_t , G can be simplified as*

$$\begin{aligned}
 G & = -\mathbb{E}_{q(y|x)} [D_{KL}(q(s|x, y)||q(s))] - \mathbb{E}_{q(y|x)} \log p(y) \\
 & = \underbrace{-I_q(s; (x, y))}_{\text{epistemic}} - \underbrace{\mathbb{E}_{q(y|x)} \log p(y)}_{\text{pragmatic}},
 \end{aligned} \tag{3}$$

where $I_q(\cdot)$ represents the mutual information given the surrogate model $q(\cdot)$.

Proof. See Appendix B. □

We can see that by construction, EFE strikes a balance between *information-seeking* and *goal-directed* behavior under some prior preferences. It bounds the difference between *epistemic* value (about parameters) and *pragmatic* value (about outcomes), which captures the imperative to maximize the epistemic value (*i.e.*, information gain about latent states), from interactions with the environment, while maximizing the pragmatic value (*i.e.*, expected preference alignment), regarding prior preferences. This crucial aspect of AIF effectively addresses the “explore-exploit dilemma” because the imperatives for exploration and exploitation are just two aspects of EFE:

Pragmatic Value (Exploitation): This term encourages goal-directed behavior by favoring actions expected to yield preferred outcomes. Encoded by a prior distribution over desired observations, it functions similarly to a utility or reward function in reinforcement learning (Millidge et al., 2020), driving the agent to exploit its current knowledge to achieve its goals.

Epistemic Value (Exploration): This term promotes information-seeking behavior by favoring actions expected

to reduce uncertainty about the underlying system maximally. It quantifies the expected information gain about the model’s parameters, driving the agent to explore the environment to refine its world model.

3.2. Reinterpretation of Acquisition Strategies in BO and BED

Crucially, minimizing EFE serves as a unifying umbrella principle. Many classic acquisition strategies in BO and BED can be reinterpreted as special cases of minimizing EFE, as shown in Table 1.

The reinterpretations of most of the acquisition strategies in Table 1 are straightforward according to their definitions. However, placing a rather intuitive GP-UCB strategy within this framework seems implicit. To reveal their connection, we rely on the following lemma:

Lemma 3.2. *Let $\mathbf{X} \subseteq \mathcal{X}$ be a subset of inputs, and the corresponding function values evaluated at those inputs be denoted as $f_{\mathbf{X}}$. Given a historical dataset \mathcal{D}_t , and new measurements \mathbf{Y} observed at \mathbf{X} , the mutual information*

$$I(f_{\mathcal{X}}; (\mathbf{X}, \mathbf{Y})|\mathcal{D}_t) = I(f_{\mathbf{X}}; \mathbf{Y}|\mathcal{D}_t),$$

for any (finite or infinite) set \mathcal{X} .

Proof. See Appendix C. □

Then if we assume constant Gaussian noises $\mathcal{N} \sim (0, \sigma^2)$ for the observations, we have

$$\begin{aligned}
 I(f_x; y|\mathcal{D}_t) & = H(y|\mathcal{D}_t) - H(y|f_x, \mathcal{D}_t) \\
 & = \frac{1}{2} \log(1 + \sigma^{-2} \sigma_t^2(x)),
 \end{aligned}$$

where $\sigma_t^2(x)$ is the variance evaluated on the GP model $p(f_x|\mathcal{D}_t)$.

When further assuming that the GP kernel $\kappa_t(x, x') \leq 1, \forall x, x' \in \mathcal{X}$, then $0 \leq \sigma_t^2(x) \leq \kappa_t(x, x') \leq 1$, which gives

$$\log(1 + \sigma^{-2} \sigma_t^2(x)) \geq \log(1 + \sigma^{-2}) \sigma_t^2(x).$$

If we choose $\beta = \frac{1}{2} \log(1 + \sigma^{-2})$, then the epistemic term in EFE, *i.e.*, $I(f_x; y|\mathcal{D}_t)$, provides an upper bound of the square of the exploration term $\beta^{1/2} \sigma_t(x)$ in GP-UCB.

This reveals the close relationship between GP-UCB and AIF, showing that even a seemingly pure intuitive strategy, like GP-UCB, can have rather rigorous mathematical foundations underlying it.

Table 1. A unified view of different acquisition strategies in BO and BED, where x^* , y^* represent the true optimal solution and value, respectively, and \hat{y} is the best value observed in \mathcal{D}_t .

Acquisition Strategy	Acquisition Function $\alpha(x)$	Expected Free Energy	
		Parameters s	Preferences $p(y)$
Expected Information Gain (Chaloner & Verdinelli, 1995)	$I(\theta; (x, y) \mathcal{D}_t)$	θ	-
Entropy Search (Hennig & Christian J. Schuler, 2012; Hernández-Lobato et al., 2014)	$I(x^*; (x, y) \mathcal{D}_t)$	x^*	-
Max-value Entropy Search (Wang & Jegelka, 2017)	$I(y^*; (x, y) \mathcal{D}_t)$	y^*	-
Joint Entropy Search (Hvarfner et al., 2022a)	$I((x^*, y^*); (x, y) \mathcal{D}_t)$	(x^*, y^*)	-
Bayesian Algorithm Execution (Neiswanger et al., 2021)	$I(\mathcal{O}_{\mathcal{A}}(f); (x, y) \mathcal{D}_t)$	$\mathcal{O}_{\mathcal{A}}(f)$	-
GP-Upper Confidence Bound	$\mu_t(x) + \beta^{1/2} \sigma_t(x)$	$f_{\mathcal{X}}$	$\exp\{y\}$
Probability of Improvement (Močkus, 1975)	$p(y \geq \hat{y})$	-	$\exp\{\mathbb{I}(y \geq \hat{y})\}$
Expected Improvement (Jones et al., 1998)	$\mathbb{E}([y - \hat{y}]_+)$	-	$\exp\{[y - \hat{y}]_+\}$

4. A New Paradigm to Derive Acquisition Functions

The preference distribution $p(y)$ in Table 1 can be interpreted as a softmax transformation of a time-varying value function over the outcomes. Generalizing from this observation, we propose a new paradigm for deriving acquisition functions applicable to a wider class of hybrid problems other than traditional BO and BED.

Grounded on *Boltzmann distribution* (also called *Gibbs distribution*) in statistical mechanics, we define an Boltzmann operator \mathcal{B}_β that maps an energy function $h(z)$ over domain \mathcal{Z} into a Boltzmann distribution:

$$(\mathcal{B}_\beta[h])(z) := \frac{e^{-h(z)/\beta}}{\int_{\mathcal{Z}} e^{-h(z)/\beta} dz},$$

where β is called a temperature parameter (in allusion to statistical mechanics). A higher temperature results in a more uniform output distribution (*i.e.* “more random” with higher entropy), while a lower temperature results in a sharper output distribution, with the maximizers of $h(z)$ dominating.

Then, for any pre-defined energy function $h(y|\mathcal{D}_t)$, we can transfer it into a Boltzmann distribution and use it as the preference distribution $p(y)$ in (3):

$$\begin{aligned} G &= -I(s; (x, y)|\mathcal{D}_t) - \mathbb{E}_{p(y|x, \mathcal{D}_t)}[\log e^{-h(y|\mathcal{D}_t)/\beta}] + Z \\ &= -I(s; (x, y)|\mathcal{D}_t) + \frac{1}{\beta} \mathbb{E}_{p(y|x, \mathcal{D}_t)}[h(y|\mathcal{D}_t)] + Z, \end{aligned}$$

where $p(y|x, \mathcal{D}_t)$ is the predictive distribution of a surrogate model constructed from the historical data \mathcal{D}_t , and

$Z = \log \int_{\mathcal{Y}} e^{-h(y|\mathcal{D}_t)/\beta} dy$ is a normalization constant independent of y .

Therefore, we propose a new acquisition paradigm, **pragmatic curiosity**, by minimizing the EFE, *i.e.*,

$$x_{t+1} = \arg \max_{x \in \mathcal{X}} \{\beta_t I(s; (x, y)|\mathcal{D}_t) - \mathbb{E}_{p(y|x, \mathcal{D}_t)}[h(y|\mathcal{D}_t)]\},$$

where $\beta_t \geq 0$ is a parameter that modulates the degree of *curiosity*, and $h(y|\mathcal{D}_t)$ is a problem-dependent energy function that captures the goal (in terms of regret w.r.t. a certain outcome y).

The curiosity β_t plays an important role in balancing the performance between learning and optimization. Li et al. (2026) derive a formal theoretical guarantee of *posterior consistency* and *bounded cumulative regret* under a *sufficient curiosity* condition, and provide practical design guidelines for choosing β_t in different settings.

This paper instead examines how a problem-dependent energy function, $h(y|\mathcal{D}_t)$, provides a flexible mechanism for explicitly representing uncertainty over the goals themselves. This added expressiveness enables acquisition design for a broad class of complex settings that standard methods often overlook, including tasks with evolving goals (where conditions change over time) and implicit goals (not specified *a priori*). The effectiveness and versatility of this formulation on such tasks are demonstrated in the next section.

5. Experiments

In this section, we exemplify the benefits and variability of the proposed acquisition strategy by performing experiments across three categories that differ substantially from

one another. These problems originate from distinct literature within BO and BED, and none of them are canonical BO or BED tasks. Thus each of them is evaluated against a different set of BO-type (optimization-focused) and BED-type (learning-focused) baselines appropriate for that specific task, ensuring a fair and rigorous comparison.

5.1. Parametric Models with Known Invariant Goals

We first consider a simplest task where the goals are known and invariant, and we have a decent understanding of the model, where only certain finite parameters are unknown.

One typical problem structure is the **constrained system identification** whose objective is to precisely learn unknown system parameters, θ , when valid observations can only be gathered under specific operational constraints, quantified by $C(y) \leq 0$. For instance, when monitoring a chemical plume, the goal is to identify its source (θ) while ensuring that sensor measurements (y) do not exceed a saturation threshold ($C(y)$).

In such cases, it is straightforward to choose the interested state as $s = \theta$, and the energy function as $h(y|\mathcal{D}_t) = \mathbb{I}(C(y) > 0)$. This leads to an acquisition function:

$$\alpha(x|\mathcal{D}_t) = \beta I(\theta; (x, y)|\mathcal{D}_t) - \mathbb{E}_{p(y|x, \mathcal{D}_t)} [\mathbb{I}(C(y) > 0)].$$

Tasks. We perform experiments on a real-world environmental monitoring problem in 2d plume fields where the sensors have a saturation threshold y_{max} (*i.e.*, $C(y) = y - y_{max}$) (Detailed settings and hyper-parameter choices in Appendix D.2). We consider three types of monitoring tasks: (a) locating the unknown source location; (b) estimating unknown wind direction and strength; and (c) identifying the active sources in fields with multiple sources.

Baselines. We compare our proposed acquisition strategy (AIF) with BO-type and BED-type baselines tailored this task: (a) Random; (b) Greedy by choosing the point that leads to the least probability of violating the constraint (BO-type); and (c) EIG about the unknown parameter (BED-type).

Evaluations. We evaluate the performance from both epistemic and pragmatic perspectives: (a) estimation accuracy; and (b) constraint violations.

Results. Fig. 1 shows that our approach achieves consistently stronger query efficiency over baselines while respecting all operational constraints, with cumulative constraint violation always being zero. This advantage is especially evident in the source localization task, where the drive for information and the need to satisfy constraints create opposing pressures. Resolving this conflict, our approach reaches near-perfect estimation using up to 40% fewer queries than competing methods.

5.2. Non-Parametric Models with Known Evolving Goals

Next, we consider a more challenging setting where the task condition evolves, and the model is fully black-box such that we need to resort to a non-parametric model (*e.g.*, GPs).

One such example is the **targeted active search** in multi-objective design problems. The objectives are viewed as metrics where specific ranges carry particular significance, and the goal is to design experiments that maximize coverage of these important regions \mathcal{S} .

Adopted from [Malkomes et al. \(2021\)](#), we assume that the experimental design problems possess a sense of known resolution, such as simulation accuracy or manufacturing precision/tolerance, and any outcome within distance δ of another does not convey extra information about \mathcal{S} . Similar to [Malkomes et al. \(2021\)](#), we define the coverage neighborhood of any y as $\mathbb{C}_\delta(y) := \{y' : d(y, y') < \delta\}$. And the coverage neighborhood of a set of points Y is defined as $\mathbb{C}_\delta(Y) := \bigcup_{y \in Y} \mathbb{C}_\delta(y)$.

Since the goal is to cover as much volume of the interested region \mathcal{S} as possible, $h(y|\mathcal{D}_t)$ can be chosen as $h(y|\mathcal{D}_t) = \text{Vol}(\mathcal{S}) - \text{Vol}(\mathbb{C}_\delta(Y \cup y) \cap \mathcal{S})$, where Y contains all the history of outcomes. Similarly, coverage over the design configurations can be flexibly incorporated by expanding the interested state into the whole input space, *i.e.*, $s = f_x$. With non-parametric models like GPs, we can leverage Lemma 3.2 and derive an acquisition function:

$$\alpha(x|\mathcal{D}_t) = \beta I(f_x; y|\mathcal{D}_t) + \mathbb{E}_{p(y|x, \mathcal{D}_t)} [\text{Vol}(\mathbb{C}_\delta(Y \cup y) \cap \mathcal{S})].$$

Tasks. We perform experiments on a real-world failure discovery problem in autonomous driving scenarios where the perception module, a YOLO detector, may fail due to multiple causes, which could potentially lead to collisions (3d input-2d output). We consider three target sets with decreasing volume, *i.e.*, Target Set 1 \supset Target Set 2 \supset Target Set 3 (Detailed settings and hyper-parameter choices in Appendix D.3).

Baselines. We again compare our proposed acquisition strategy (AIF) with BO-type and BED-type baselines tailored this task: (a) Random; (b) Greedy by maximizing coverage volume in metrics space (BO-type); and (c) EIG by maximizing coverage volume in parameter space (BED-type).

Evaluations. We evaluate the performance by inspecting the coverage volume over both spaces: (a) metrics space ($\mathbb{C}_\delta(Y)$); and (b) parameter space ($\mathbb{C}_\delta(X)$).

Results. As shown in Fig. 2, our AIF algorithm effectively balances coverage of both the parameter and metrics spaces. This capability is especially impactful for smaller target sets where the search is more difficult. In the most challenging case (Target Set 3), our method identifies nearly 10%

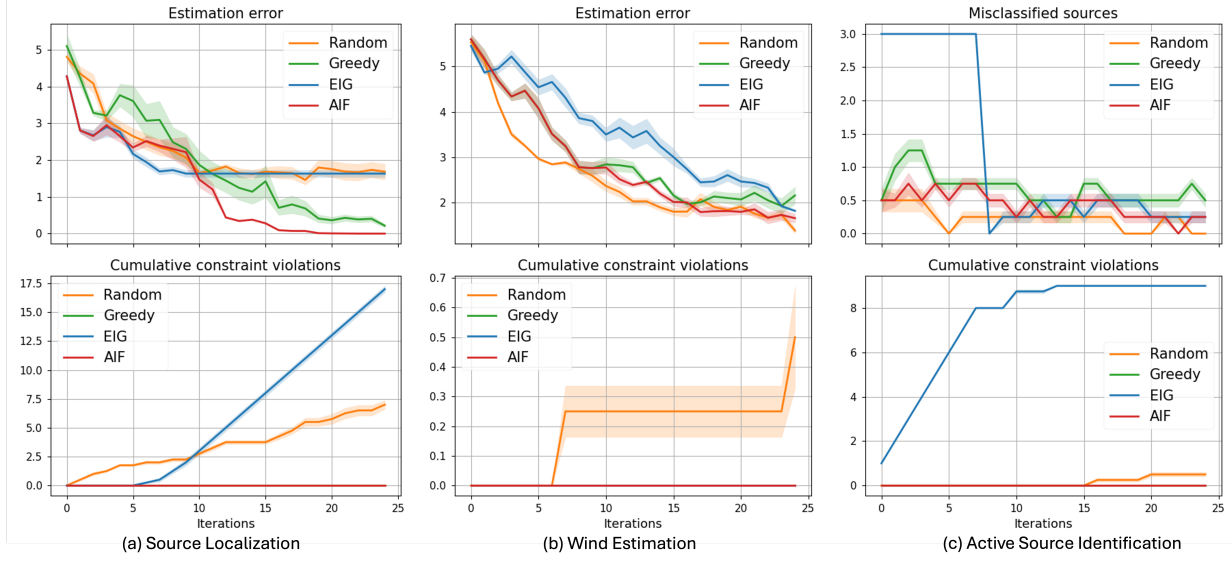


Figure 1. Performance evaluation for constrained system identification on environmental monitoring in 2d plume fields. Error bars represent ± 1 std over 5 seeds.

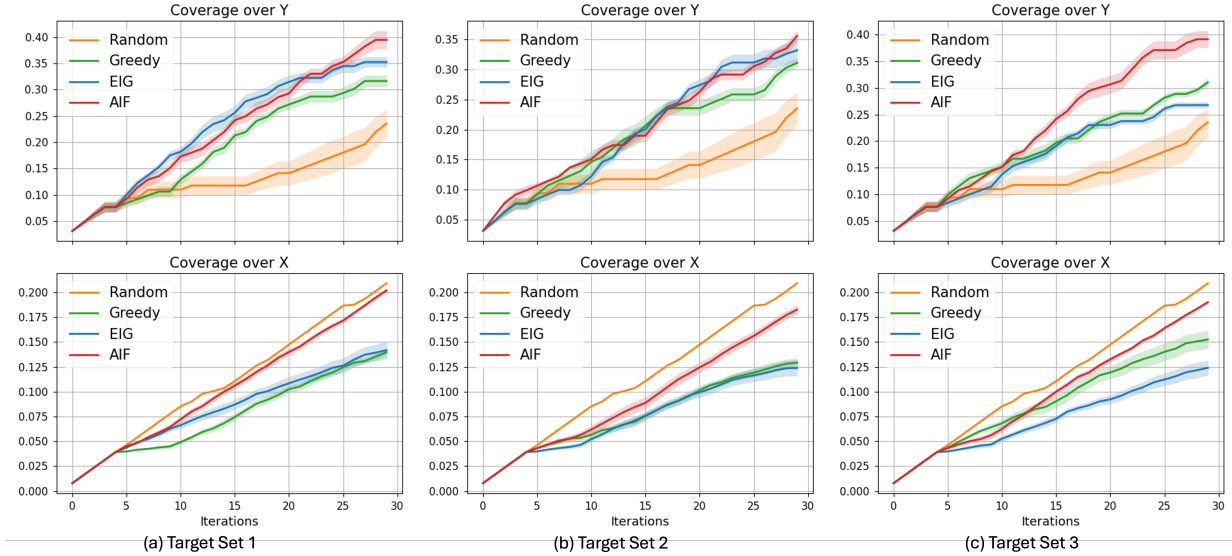


Figure 2. Performance evaluation for targeted active search on failure discovery in autonomous driving scenarios. Error bars represent ± 1 std over 4 seeds.

more of the critical failure region compared to the leading baseline.

5.3. Non-Parametric Models with Unknown Goals

Finally, we look into the most difficult setting where both the models and goals are black-box.

One practical scenario arises from the **composite Bayesian optimization** in multi-objective optimization problems. The objectives are weighted by a preference function $g(y)$ that is unknown *a priori* and must be simultaneously learned

during the optimization process.

As assumed in Lin et al. (2022), we can estimate the unknown preference function $g(y)$ by asking a decision-maker (DM) to express preferences over pairs of outcomes (y_1, y_2) . Let $z(y_1, y_2) \in \{1, 2\}$ indicate whether the DM preferred the first or second outcome offered. Following Chu & Ghahramani (2005), we assume that the DM's responses are distributed according to a *probit* likelihood: $L(z(y_1, y_2) = 1 | g(y_1), g(y_2)) = \Phi(\frac{g(y_1) - g(y_2)}{\sqrt{2}\lambda})$, where λ is a hyperparameter, and Φ is the standard normal CDF.

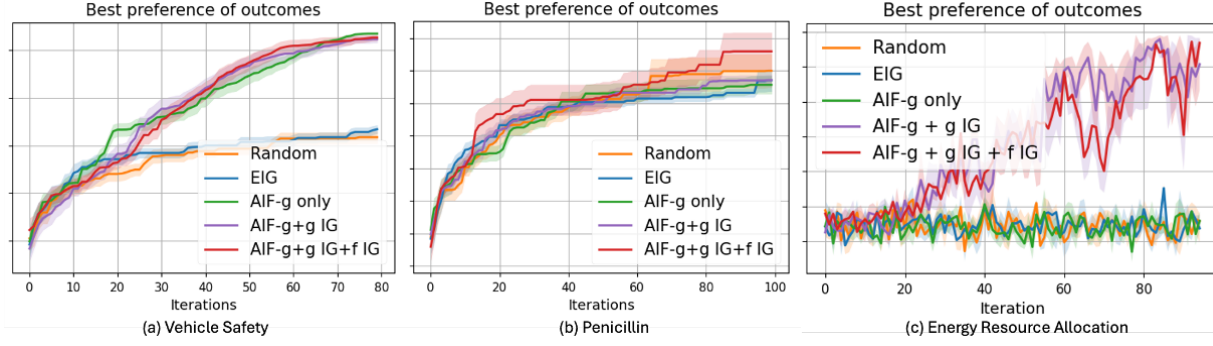


Figure 3. Performance evaluation for composite BO with unknown preferences. Error bars represent ± 1 std over 20 seeds for vehicle safety, penicillin, and 5 for energy resource allocation.

Taking the joint exploration and exploitation of the preference function $g(y)$ into consideration, we can choose $h(y|\mathcal{D}_t)$ as the EFE of the preference model, *i.e.*, $h(y|\mathcal{D}_t) = \text{EFE}(g(y))$, which naturally extends the acquisition function into a nested structure:

$$\alpha(x|\mathcal{D}_t) = \gamma I(f_x; y|\mathcal{D}_t) + \mathbb{E}_{p(y|x, \mathcal{D}_t)} [\beta I(g_y; z|\mathcal{D}_t) + \mathbb{E}_{p(g_y|y, \mathcal{D}_t)} g_y], \quad (4)$$

where $x = [x_1, x_2]$ are two jointly evaluated candidates, and $\gamma, \beta \geq 0$.

Tasks. We perform experiments on three real-world problems, including vehicle safety (5d-3d), penicillin production simulator (7d-3d), and distributed energy resource allocation in power grids (40d-4d) (Detailed settings and hyperparameter choices in Appendix D.4).

Baselines. Different from BOPE in Lin et al. (2022), which separates and iterates the *preference exploration* and *experimentation* stages, our approach unifies the exploration and exploitation of both outcome and preference models simultaneously. In its best setting (*i.e.*, switch stages and update models at each step), their acquisition strategy reduces to a special case of our proposed (4) with $\beta = \gamma = 0$. Thus, we design a set of baselines to investigate the effect that each component in (4) plays for the joint exploration and exploitation of hierarchical models. We ablate the full AIF strategy ($g + g \text{ IG} + f \text{ IG}$) by (a) removing the last term (EIG); (b) removing the first term ($g + g \text{ IG}$); and (c) removing the first two terms (g only).

Evaluations. We evaluate their performance by inspecting the best preference of all collected outcomes using the true preference function $g(y)$.

Results. Fig. 3 illustrates our AIF approach’s outstanding ability to learn unknown preference functions, a key advantage over baselines that often fail due to ill-directed queries. As the tasks become more complex and noisy (from (a) to (c)), our results demonstrate that every component of our

acquisition function (4) plays an irreplaceable role in achieving optimal performance. This benefit is most stark in the energy resource allocation task, where competing methods failed to capture any meaningful preference model while our approach consistently succeeded.

Benefits of joint learning and optimization. To highlight the benefits of jointly learning and optimizing, rather than separating these into stages, we compare our method against several BOPE variants from Lin et al. (2022) that use different stage-wise design choices. Detailed experimental setups, design choices, plots, and analyses are provided in Appendix D.4.3. The results show that our method naturally balances exploration and exploitation at each step and consistently discovers higher-preference regions, whereas the BOPE variants are highly sensitive to how the stages are configured. Consequently, stage-wise approaches like BOPE require careful manual tuning of these choices, while our unified formulation automates this trade-off and is therefore more amenable to higher-order hierarchical models.

6. Conclusion and Limitation

We presented *pragmatic curiosity*, an AIF-based paradigm for hybrid learning-optimization under expensive black-box evaluations. By selecting actions via EFE minimization, the approach unifies goal-seeking and information-seeking within a single acquisition objective. Across constrained system identification, targeted active search, and composite optimization with unknown preferences, pragmatic curiosity consistently outperformed strong BO-type and BED-type baselines, improving estimation accuracy, critical-region coverage, and final solution quality under fixed budgets.

The limitation of our approach stems from the specification of the problem-dependent energy/preference model; misspecification can bias acquisition and degrade performance. Performance also inherits assumptions of the underlying surrogate and observation models; strong model mismatch or non-stationarity can compromise both uncertainty quan-

tification and preference-induced guidance. Future work includes extending the evaluation of this paradigm to multi-agent, long-horizon, or multi-fidelity settings.

Impact Statement

This work advances sample-efficient decision-making for engineering and scientific systems where evaluations are expensive and objectives are coupled to uncertainty. By unifying goal-seeking and information-seeking within a single EFE objective, *pragmatic curiosity* provides a general acquisition-design template that can reduce experimental cost, accelerate discovery, and improve reliability in workflows such as safe system identification, targeted failure-region discovery, and preference-driven design. In domains like environmental monitoring, autonomous-system testing, and energy-resource allocation, the practical benefit is fewer costly or risky evaluations for a given level of performance and confidence, which can translate into reduced resource consumption and safer experimentation.

Potential negative impacts stem from misuse or mispecification of the preference/energy model: poorly chosen goals or biased preferences can steer exploration toward harmful regions (e.g., unsafe operating conditions) or encode inequitable outcomes in preference-driven optimization. In addition, the ability to more efficiently identify system vulnerabilities could be misused in adversarial settings. These risks motivate careful deployment practices, including explicit safety constraints, transparent preference specification, robustness checks under model mismatch, and domain-appropriate oversight when the method is applied to safety-critical or socially sensitive applications.

References

Bakshy, E., Dworkin, L., Karrer, B., Kashin, K., Letham, B., Murthy, A., and Singh, S. AE: A domain-agnostic platform for adaptive experimentation. In *Conference on neural information processing systems*, pp. 1–8, 2018.

Balandat, M., Karrer, B., Jiang, D. R., Daulton, S., Letham, B., Wilson, A. G., and Bakshy, E. BoTorch: A Framework for Efficient Monte-Carlo Bayesian Optimization. *Advances in neural information processing systems*, 33: 21524–21538, 10 2020.

Chaloner, K. and Verdinelli, I. Bayesian experimental design: A review. *Statistical science*, pp. 273–304, 1995.

Chu, W. and Ghahramani, Z. Preference learning with Gaussian processes. In *Proceedings of the 22nd international conference on Machine learning*, pp. 137–144, 2005.

Coelho, R. C., Alves, A. F. C., Pires, T. N., and Pires, F. A. A composite bayesian optimisation framework for material and structural design. *Computer Methods in Applied Mechanics and Engineering*, 434:117516, 2025.

Di Fiore, F., Nardelli, M., and Mainini, L. Active learning and bayesian optimization: A unified perspective to learn with a goal. *arXiv preprint arXiv:2303.01560*, 2023.

Dosovitskiy, A., Ros, G., Codevilla, F., Lopez, A., and Koltun, V. CARLA: An open urban driving simulator. In *Conference on robot learning*, pp. 1–16, 2017.

Dreossi, T., Fremont, D. J., Ghosh, S., Kim, E., Ravanbakhsh, H., Vazquez-Chanlatte, M., and Seshia, S. A. Verifai: A toolkit for the formal design and analysis of artificial intelligence-based systems. In *International Conference on Computer Aided Verification*, pp. 432–442, 2019.

Frazier, P. I. A Tutorial on Bayesian Optimization. (Section 5):1–22, 2018. URL <http://arxiv.org/abs/1807.02811>.

Fremont, D. J., Dreossi, T., Ghosh, S., Yue, X., Sangiovanni-Vincentelli, A. L., and Seshia, S. A. Scenic: a language for scenario specification and scene generation. In *Proceedings of the 40th ACM SIGPLAN conference on programming language design and implementation*, pp. 63–78, 2019.

Friston, K. The free-energy principle: A unified brain theory?, 2 2010. ISSN 1471003X.

Friston, K., FitzGerald, T., Rigoli, F., Schwartenbeck, P., and Pezzulo, G. Active Inference: A Process Theory. *Neural Computation*, 29(1):1–49, 1 2017. ISSN 0899-7667. doi: 10.1162/NECO{_}a{_}00912.

Friston, K. J., Ramstead, M. J., Kiefer, A. B., Tschantz, A., Buckley, C. L., Albarracin, M., Pitliya, R. J., Heins, C., Klein, B., Millidge, B., Sakthivadivel, D. A., St Clere Smithe, T., Koudahl, M., Tremblay, S. E., Petersen, C., Fung, K., Fox, J. G., Swanson, S., Mapes, D., and René, G. Designing ecosystems of intelligence from first principles. *Collective Intelligence*, 3(1), 1 2024. ISSN 2633-9137. doi: 10.1177/26339137231222481.

Gardner, J. R., Pleiss, G., Bindel, D., Weinberger, K. Q., and Wilson, A. G. GPyTorch: Blackbox Matrix-Matrix Gaussian Process Inference with GPU Acceleration. *Advances in neural information processing systems*, 31, 9 2018.

González, L. D. and Zavala, V. M. Implementation of a bayesian optimization framework for interconnected systems. *Industrial & Engineering Chemistry Research*, 64 (4):2168–2182, 2025.

Hennig, P. and Christian J. Schuler. Entropy search for information-efficient global optimization. *Journal of Machine Learning Research*, 13(6), 2012.

Hernández-Lobato, J. M., Hoffman, W. M., and Ghahramani, Z. Predictive entropy search for efficient global optimization of black-box functions. In *Advances in neural information processing systems*, 2014.

Hvorfner, C., Hutter, F., and Nardi, L. Joint Entropy Search for Maximally-Informed Bayesian Optimization. 6 2022a. URL <http://arxiv.org/abs/2206.04771>.

Hvorfner, C., Hutter, F., and Nardi, L. Joint entropy search for maximally-informed bayesian optimization. *Advances in Neural Information Processing Systems*, 35:11494–11506, 2022b.

Hvorfner, C., Hellsten, E., Hutter, F., and Nardi, L. Self-Correcting Bayesian Optimization through Bayesian Active Learning. In *Conference on Neural Information Processing Systems (NeurIPS)*, 2 2023. URL <http://arxiv.org/abs/2304.11005>.

Hvorfner, C., Eriksson, D., Bakshy, E., and Balandat, M. Informed initialization for bayesian optimization and active learning. *arXiv preprint arXiv:2510.23681*, 2025.

Jiang, P., Ergu, D., Liu, F., Cai, Y., and Ma, B. A Review of Yolo algorithm developments. *Procedia computer science*, 199:1066–1073, 2022.

Jones, D. R., Schonlau, M., and Welch, W. J. Efficient Global Optimization of Expensive Black-Box Functions. *Journal of Global Optimization*, 13(4):455–492, 1998. ISSN 09255001. doi: 10.1023/A:1008306431147.

Kianmehr, E., Nikkhah, S., Vahidinasab, V., Giaouris, D., and Taylor, P. C. A Resilience-Based Architecture for Joint Distributed Energy Resources Allocation and Hourly Network Reconfiguration. *IEEE Transactions on Industrial Informatics*, 15(10):5444–5455, 10 2019. ISSN 1551-3203. doi: 10.1109/TII.2019.2901538.

Konakovic Lukovic, M., Tian, Y., and Matusik, W. Diversity-guided multi-objective bayesian optimization with batch evaluations. In *Advances in Neural Information Processing Systems*, pp. 17708–17720, 2020.

Lanillos, P., Meo, C., Pezzato, C., Meera, A. A., Baioumy, M., Ohata, W., Tschantz, A., Millidge, B., Wisse, M., Buckley, C. L., and Tani, J. Active Inference in Robotics and Artificial Agents: Survey and Challenges. 12 2021. URL <http://arxiv.org/abs/2112.01871>.

Li, Y., Parashar, A., Zhou, E., and Fan, C. Curiosity is knowledge: Self-consistent learning and no-regret optimization with active inference. *arXiv preprint*, 2026.

Liang, Q. and Lai, L. Scalable bayesian optimization accelerates process optimization of penicillin production. In *NeurIPS 2021 AI for Science Workshop*, 2021.

Lin, Z. J., Astudillo, R., Frazier, P. I., and Bakshy, E. Preference Exploration for Efficient Bayesian Optimization with Multiple Outcomes. In *International Conference on Artificial Intelligence and Statistics*, pp. 4235–4258, 3 2022. URL <http://arxiv.org/abs/2203.11382>.

Lookman, T., Balachandran, P. V., Xue, D., and Yuan, R. Active learning in materials science with emphasis on adaptive sampling using uncertainties for targeted design. *npj Computational Materials*, 5(1):21, 2019.

Malkomes, G., Cheng, B., Lee, E. H., and McCourt, M. Beyond the Pareto Efficient Frontier: Constraint Active Search for Multiobjective Experimental Design. *Technical report*, 2021.

Matsumoto, T., Fujii, K., Murata, S., and Tani, J. Active inference with dynamic planning and information gain in continuous space by inferring low-dimensional latent states. *Entropy*, 27(8):846, 2025.

Millidge, B., Tschantz, A., Seth, A. K., and Buckley, C. L. On the relationship between active inference and control as inference. In *Communications in Computer and Information Science*, volume 1326, pp. 3–11. Springer Science and Business Media Deutschland GmbH, 2020. ISBN 9783030649180. doi: 10.1007/978-3-030-64919-7__1.

Močkus, J. On Bayesian Methods for Seeking the Extremum. In *Optimization Techniques IFIP Technical Conference*, pp. 400–404. Springer Berlin Heidelberg, Berlin, Heidelberg, 1975. doi: 10.1007/978-3-662-38527-2__55.

Neiswanger, W., Wang, K. A., and Ermon, S. Bayesian algorithm execution: Estimating computable properties of black-box functions using mutual information. In *International Conference on Machine Learning*, pp. 8005–8015, 2021.

Rainforth, T., Foster, A., Ivanova, D. R., and Smith, F. B. Modern Bayesian Experimental Design. 2 2023. URL <http://arxiv.org/abs/2302.14545>.

Ramanagopal, M. S., Anderson, C., Vasudevan, R., and Johnson-Roberson, M. Failing to Learn: Autonomously Identifying Perception Failures for Self-Driving Cars. *IEEE Robotics and Automation Letters*, 3(4):3860–3867, 10 2018. ISSN 2377-3766. doi: 10.1109/LRA.2018.2857402.

Redmon, J. and Farhadi, A. YOLOv3: An Incremental Improvement. *arXiv preprint arXiv:1804.02767*, 4 2018.

Russo, D. and Van Roy, B. Learning to Optimize via Information-Directed Sampling. *Operations Research*, 66(1):230–252, 2 2018. ISSN 0030-364X. doi: 10.1287/opre.2017.1663. URL <https://pubsonline.informs.org/doi/10.1287/opre.2017.1663>.

Schervish, M. J. *Theory of Statistics*. Springer New York, New York, NY, 1995. ISBN 978-1-4612-8708-7. doi: 10.1007/978-1-4612-4250-5.

Shahriari, B., Swersky, K., Wang, Z., Adams, R. P., and De Freitas, N. Taking the human out of the loop: A review of Bayesian optimization. *Proceedings of the IEEE*, 104(1):148–175, 2016. ISSN 15582256. doi: 10.1109/JPROC.2015.2494218.

Smith, F. B., Kirsch, A., Farquhar, S., Gal, Y., Foster, A., and Rainforth, T. Prediction-Oriented Bayesian Active Learning. In *International Conference on Artificial Intelligence and Statistics (AISTATS)*, 2023.

Smith, R., Friston, K. J., and Whyte, C. J. A step-by-step tutorial on active inference and its application to empirical data. *Journal of Mathematical Psychology*, 107, 4 2022. ISSN 10960880. doi: 10.1016/j.jmp.2021.102632.

Tanabe, R. and Ishibuchi, H. An Easy-to-use Real-world Multi-objective Optimization Problem Suite. 9 2020. doi: 10.1016/j.asoc.2020.106078.

Titsias, M. Variational learning of inducing variables in sparse Gaussian processes. In *Artificial intelligence and statistics*, pp. 567–574, 2009.

Tu, B., Gandy, A., Kantas, N., and Shafei, B. Joint entropy search for multi-objective bayesian optimization. *Advances in Neural Information Processing Systems*, 35: 9922–9938, 2022.

Wang, J., Yang, Z., Hu, X., Li, L., Lin, K., Gan, Z., Liu, Z., Liu, C., and Wang, L. GIT: A Generative Image-to-text Transformer for Vision and Language. 5 2022.

Wang, Z. and Jegelka, S. Max-value entropy search for efficient Bayesian optimization. In *International Conference on Machine Learning*, pp. 3627–3635, 2017.

Wilson, J. T., Hutter, F., and Deisenroth, M. P. Maximizing acquisition functions for Bayesian optimization. In *Conference on Neural Information Processing Systems (NeurIPS)*, 12 2018. URL <http://arxiv.org/abs/1805.10196>.

Zhong, M., Tran, K., Min, Y., Wang, C., Wang, Z., Dinh, C.-T., De Luna, P., Yu, Z., Rasouli, A. S., Brodersen, P., Sun, S., Voznyy, O., Tan, C.-S., Askerka, M., Che, F., Liu, M., Seifitokaldani, A., Pang, Y., Lo, S.-C., Ip, A., Ulissi, Z., and Sargent, E. H. Accelerated discovery of CO₂ electrocatalysts using active machine learning. *Nature*, 581(7807):178–183, 5 2020. ISSN 0028-0836. doi: 10.1038/s41586-020-2242-8.

A. Related Work

Several independent attempts have been made to handle the hybrid objectives of goal seeking and learning. Below, we discuss some key prior works, originating from three viewpoints: (1) BO-based settings, (2) BED (also known as Bayesian active learning, BAL) based works, and (3) some works that have acknowledged the synergy and attempted to present a unifying viewpoint, using adaptive sampling and AIF-based approaches.

On the BO side, [Russo & Van Roy \(2018\)](#) proposed information-directed sampling (IDS) to online optimization problems by minimizing the ratio between squared expected single-period regret and a measure of information gain. [Hvarfner et al. \(2023\)](#) introduced a statistical distance-based active learning (SAL) criterion into the BO loop to actively learn the Gaussian process hyperparameter even as it searches for the optimum. [Tu et al. \(2022\)](#); [Hvarfner et al. \(2022b\)](#) propose an information-theoretic acquisition function for multi-objective BO, which considers the joint information gain for the optimal set of inputs and outputs. Overall, these works acknowledge and demonstrate the value of information gain in enhancing the capabilities of goal-seeking strategies, with an ultimate focus on optimization. However, they do not explicitly comment on the synergy of goal seeking and learning, or formalize the acquisition strategies as a way to explicitly balance both objectives.

On the BED (also known as Bayesian active learning, BAL) side, [Smith et al. \(2023\)](#) proposed an expected predictive information gain (EPIG) criterion that focuses on information gain in model predictions, mitigating classical BAL's tendency to select out-of-distribution or low-relevance queries by accounting for an input data distribution. [Lookman et al. \(2019\)](#) discusses the performance of various BAL and BO strategies for material design application, noting their connection with adaptive sampling, and simultaneous exploration and exploitation. This shows that the realistic application of BO/BED-based approaches often necessitates a formalized viewpoint unifying each distinct objective.

These efforts begin to show the growing synergy between BO and BED techniques, where information-gain criteria are leveraged to enhance optimization and vice versa. In search of a unifying perspective for these techniques, [Di Fiore et al. \(2023\)](#) views BO and BAL as symbiotic adaptive sampling techniques driven by common principles of ‘goal-driven learning’. However, their viewpoint is limited to BO and BED as separate realizations of adaptive sampling, and they do not discuss a way to combine both objectives in a single acquisition strategy.

In this paper, we present a unified perspective that arises naturally from the principles of Active Inference (AIF) ([Friston, 2010](#); [Friston et al., 2017](#)). Originally developed in computational neuroscience, AIF has been successfully applied in fields such as robotics ([Lanillos et al., 2021](#)), cognitive science ([Smith et al., 2022](#)), ecosystem modeling ([Friston et al., 2024](#)), and goal-directed planning in partially observable environments ([Matsumoto et al., 2025](#)). These works leverage the ability of AIF to accommodate goal-directed and epistemic considerations, which we utilize as the backbone for our unifying mechanism discussed in this paper.

B. Proof of Theorem 3.1

Proof. Recall that

$$G = \underbrace{-\mathbb{E}_{q(y,s|x)} [\log p(s|x, y) - \log q(s|x)]}_{\text{Term 1}} - \underbrace{\mathbb{E}_{q(y|x)} \log p(y|x)}_{\text{Term 2}}$$

Since our purpose is to align the true outcome distribution given the decision x (*i.e.*, $p(y|x)$) with the prior preference distribution $p(y)$, we replace the second term of G by $-\mathbb{E}_{q(y|x)} \log p(y)$. It is commonly referred to as *pragmatic* value, which scores the anticipated surprisal of the future outcomes given a predictive distribution $q(y|x)$.

For the first term of G , add and subtract $\log q(s|x, y)$ inside the expectation, we get

$$\begin{aligned} \text{Term 1} &= -\mathbb{E}_{q(y,s|x)} [\log p(s|x, y) - \log q(s|x, y) + \log q(s|x, y) - \log q(s|x)] \\ &= -\mathbb{E}_{q(y|x)} \mathbb{E}_{q(s|x,y)} [\log p(s|x, y) - \log q(s|x, y) + \log q(s|x, y) - \log q(s|x)] \\ &= -\mathbb{E}_{q(y|x)} [\mathbb{E}_{q(s|x,y)} [\log p(s|x, y) - \log q(s|x, y)] + \mathbb{E}_{q(s|x,y)} [\log q(s|x, y) - \log q(s|x)]] \\ &= -\mathbb{E}_{q(y|x)} \left[\underbrace{-D_{\text{KL}}(q(s|x, y) || p(s|x, y))}_{\text{Term 3}} + \underbrace{D_{\text{KL}}(q(s|x, y) || q(s|x))}_{\text{Term 4}} \right]. \end{aligned} \tag{5}$$

Since the surrogate model $q(s)$ usually will not be updated until a new outcome y is observed, it doesn't depend on the

decision variable x solely, *i.e.*, $q(s|x) = q(s)$. Thus Term 4 becomes $D_{\text{KL}}(q(s|x, y) || q(s))$, which is commonly referred to as the *epistemic* value, or the expected information gain of a state when it is conditioned on expected observations.

Term 3 is, in general, intractable since it depends on the true posterior distribution $p(s|x, y)$ that is often unknown. The best surrogate model we can have is $q(\cdot) = p(\cdot | \mathcal{D}_t)$ that is constructed from all available data \mathcal{D}_t . Thus if we treat this surrogate model $q(s)$ as the best approximation of the true model $p(s)$, *i.e.*, $q(s) \approx p(s)$, and the surrogate and true models both follow the Bayes' rule, *i.e.*, $q(s|x, y) = \frac{p(x, y|s)q(s)}{\int p(x, y|s)q(s)ds}$, $p(s|x, y) = \frac{p(x, y|s)p(s)}{\int p(x, y|s)p(s)ds}$, then Term 3 vanishes. \square

C. Proof of Lemma 3.2

To prove Lemma 3.2, we first introduce a lemma:

Lemma C.1. *For any (finite or infinite) set \mathcal{X} , after a few new measurements (\mathbf{X}, \mathbf{Y}) , $\mathbf{X} \subseteq \mathcal{X}$ the KL divergence between $p(f_{\mathcal{X}}|\mathcal{D} \cup (\mathbf{X}, \mathbf{Y}))$ and $p(f_{\mathcal{X}}|\mathcal{D})$ is*

$$D_{\text{KL}}[p(f_{\mathcal{X}}|\mathcal{D} \cup (\mathbf{X}, \mathbf{Y})) || p(f_{\mathcal{X}}|\mathcal{D})] = \mathbb{E}_{p(f_{\mathbf{X}}|\mathcal{D})} \left[\frac{L(\mathbf{Y}|f_{\mathbf{X}})}{L(\mathbf{Y})} \log \frac{L(\mathbf{Y}|f_{\mathbf{X}})}{L(\mathbf{Y})} \right],$$

where $L(\mathbf{Y}|f_{\mathbf{X}})$ is the likelihood of observations, $L(\mathbf{Y}) = \int L(\mathbf{Y}|f_{\mathbf{X}})p(f_{\mathbf{X}}|\mathcal{D})df_{\mathbf{X}}$ the marginal likelihood.

Proof. We first consider the case where \mathcal{X} is *finite* to provide an intuitive insight. The KL divergence between $p(f_{\mathcal{X}}|\mathcal{D} \cup (\mathbf{X}, \mathbf{Y}))$ and $p(f_{\mathcal{X}}|\mathcal{D})$ can be given as

$$\begin{aligned} & D_{\text{KL}}[p(f_{\mathcal{X}}|\mathcal{D} \cup (\mathbf{X}, \mathbf{Y})) || p(f_{\mathcal{X}}|\mathcal{D})] \\ &= D_{\text{KL}}[p(f_{\mathcal{X} \setminus \mathbf{X}}, f_{\mathbf{X}}|\mathcal{D} \cup (\mathbf{X}, \mathbf{Y})) || p(f_{\mathcal{X} \setminus \mathbf{X}}, f_{\mathbf{X}}|\mathcal{D})] \\ &= \int p(f_{\mathcal{X} \setminus \mathbf{X}}, f_{\mathbf{X}}|\mathcal{D} \cup (\mathbf{X}, \mathbf{Y})) \log \frac{p(f_{\mathcal{X} \setminus \mathbf{X}}, f_{\mathbf{X}}|\mathcal{D} \cup (\mathbf{X}, \mathbf{Y}))}{p(f_{\mathcal{X} \setminus \mathbf{X}}, f_{\mathbf{X}}|\mathcal{D})} df_{\mathcal{X} \setminus \mathbf{X}} df_{\mathbf{X}} \\ &= \int p(f_{\mathcal{X} \setminus \mathbf{X}}, f_{\mathbf{X}}|\mathcal{D} \cup (\mathbf{X}, \mathbf{Y})) \log \frac{p(f_{\mathcal{X} \setminus \mathbf{X}}, f_{\mathbf{X}}|\mathcal{D})L(\mathbf{Y}|f_{\mathbf{X}})}{p(f_{\mathcal{X} \setminus \mathbf{X}}, f_{\mathbf{X}}|\mathcal{D})L(\mathbf{Y})} df_{\mathcal{X} \setminus \mathbf{X}} df_{\mathbf{X}} \\ &= \int p(f_{\mathcal{X} \setminus \mathbf{X}}, f_{\mathbf{X}}|\mathcal{D} \cup (\mathbf{X}, \mathbf{Y})) \log \frac{L(\mathbf{Y}|f_{\mathbf{X}})}{L(\mathbf{Y})} df_{\mathcal{X} \setminus \mathbf{X}} df_{\mathbf{X}} \\ &= \int p(f_{\mathbf{X}}|\mathcal{D} \cup (\mathbf{X}, \mathbf{Y})) \log \frac{L(\mathbf{Y}|f_{\mathbf{X}})}{L(\mathbf{Y})} df_{\mathbf{X}} \\ &= \int \frac{p(f_{\mathbf{X}}|\mathcal{D})L(\mathbf{Y}|f_{\mathbf{X}})}{L(\mathbf{Y})} \log \frac{L(\mathbf{Y}|f_{\mathbf{X}})}{L(\mathbf{Y})} df_{\mathbf{X}} \\ &= \mathbb{E}_{p(f_{\mathbf{X}}|\mathcal{D})} \left[\frac{L(\mathbf{Y}|f_{\mathbf{X}})}{L(\mathbf{Y})} \log \frac{L(\mathbf{Y}|f_{\mathbf{X}})}{L(\mathbf{Y})} \right], \end{aligned} \tag{6}$$

where $L(\mathbf{Y}|f_{\mathbf{X}})$ is the likelihood of observations, $L(\mathbf{Y}) = \int L(\mathbf{Y}|f_{\mathbf{X}})p(f_{\mathbf{X}}|\mathcal{D})df_{\mathbf{X}}$ the marginal likelihood.

Now we move to the more general cases where \mathcal{X} is *infinite*. In such cases, there is no useful infinite-dimensional Lebesgue measure with respect to an “infinite-dimensional vector” $f_{\mathcal{X}}$. Thus, we need to resort to a more general definition for KL divergence based on the Radon-Nikodym derivative:

Definition C.2. If P and Q are probability measures over a set \mathcal{X} , and P is absolutely continuous with respect to Q , then the KL divergence from P to Q is defined as

$$D_{\text{KL}}[P || Q] = \int_{\mathcal{X}} \log\left(\frac{dP}{dQ}\right) dP,$$

where $\frac{dP}{dQ}$ is the Radon-Nikodym derivative of P with respect to Q , and provided the expression on the right-hand side exists.

According to the measure-theoretic definition of Bayes' theorem for a dominated model (Schervish, 1995), the Radon-Nikodym derivative of the posterior $P(\cdot) := p(\cdot | \mathcal{D} \cup (\mathbf{X}, \mathbf{Y}))$ with respect to the prior $\hat{P}(\cdot) := p(\cdot | \mathcal{D})$ is given as

$$\frac{dP}{d\hat{P}}(f_{\mathcal{X}}) = \frac{L(\mathbf{Y}|f_{\mathcal{X}})}{L(\mathbf{Y})}.$$

Since the dataset \mathbf{Y} is finite, so similar to previous, we restrict the likelihood to only depend on the finite dataset:

$$\frac{dP}{d\hat{P}}(f_{\mathcal{X}}) = \frac{L(\mathbf{Y}|f_{\mathbf{X}})}{L(\mathbf{Y})}.$$

Now the KL divergence between \hat{P} and P is quantified as

$$\begin{aligned} & D_{\text{KL}}[P(f_{\mathcal{X}}) \parallel \hat{P}(f_{\mathcal{X}})] \\ &= \int_{f_{\mathcal{X}}} \log\left(\frac{dP}{d\hat{P}}(f_{\mathcal{X}})\right) dP(f_{\mathcal{X}}) \\ &= \int_{f_{\mathcal{X}}} \log\left(\frac{L(\mathbf{Y}|f_{\mathbf{X}})}{L(\mathbf{Y})}\right) dP(f_{\mathcal{X}}) \\ &= \int_{f_{\mathcal{X}}} \log\left(\frac{L(\mathbf{Y}|f_{\mathbf{X}})}{L(\mathbf{Y})}\right) \frac{L(\mathbf{Y}|f_{\mathbf{X}})}{L(\mathbf{Y})} d\hat{P}(f_{\mathcal{X}}) \\ &= \int_{f_{\mathbf{X}}} \log\left(\frac{L(\mathbf{Y}|f_{\mathbf{X}})}{L(\mathbf{Y})}\right) \frac{L(\mathbf{Y}|f_{\mathbf{X}})}{L(\mathbf{Y})} d\hat{P}(f_{\mathbf{X}}) \\ &= \mathbb{E}_{\hat{P}(f_{\mathbf{X}})} \left[\frac{L(\mathbf{Y}|f_{\mathbf{X}})}{L(\mathbf{Y})} \log \frac{L(\mathbf{Y}|f_{\mathbf{X}})}{L(\mathbf{Y})} \right], \end{aligned} \tag{7}$$

which has the exact same form as (6).

Therefore, we can conclude that regardless of the set \mathcal{X} being finite or infinite, the KL divergence between the prior and posterior only depends on the evaluations of the observed data. That is to say, whilst we are in fact quantifying the KL divergence between the full distributions, we only need to keep track of the distribution over finite function values $f_{\mathbf{X}}$. \square

Now we are ready to prove Lemma 3.2.

Proof. According to Lemma C.1,

$$\begin{aligned} I(f_{\mathcal{X}}; (\mathbf{X}, \mathbf{Y}) | \mathcal{D}) &= \mathbb{E}_{p(\mathbf{Y}|\mathbf{X}, \mathcal{D})} [D_{\text{KL}}[p(f_{\mathcal{X}}|\mathcal{D} \cup (\mathbf{X}, \mathbf{Y})) \parallel p(f_{\mathcal{X}}|\mathcal{D})]] \\ &= \mathbb{E}_{p(\mathbf{Y}|\mathbf{X}, \mathcal{D})} \mathbb{E}_{p(f_{\mathbf{X}}|\mathcal{D})} \left[\frac{L(\mathbf{Y}|f_{\mathbf{X}})}{L(\mathbf{Y})} \log \frac{L(\mathbf{Y}|f_{\mathbf{X}})}{L(\mathbf{Y})} \right] \\ &= \mathbb{E}_{L(\mathbf{Y})} \mathbb{E}_{p(f_{\mathbf{X}}|\mathcal{D})} \left[\frac{L(\mathbf{Y}|f_{\mathbf{X}})}{L(\mathbf{Y})} \log \frac{L(\mathbf{Y}|f_{\mathbf{X}})}{L(\mathbf{Y})} \right] \\ &= \mathbb{E}_{p(f_{\mathbf{X}}|\mathcal{D})} \mathbb{E}_{L(\mathbf{Y})} \left[\frac{L(\mathbf{Y}|f_{\mathbf{X}})}{L(\mathbf{Y})} \log \frac{L(\mathbf{Y}|f_{\mathbf{X}})}{L(\mathbf{Y})} \right] \\ &= \mathbb{E}_{p(f_{\mathbf{X}}|\mathcal{D})} \int \left[\frac{L(\mathbf{Y}|f_{\mathbf{X}})}{L(\mathbf{Y})} \log \frac{L(\mathbf{Y}|f_{\mathbf{X}})}{L(\mathbf{Y})} \right] L(\mathbf{Y}) d\mathbf{Y} \\ &= \mathbb{E}_{p(f_{\mathbf{X}}|\mathcal{D})} \int L(\mathbf{Y}|f_{\mathbf{X}}) \log \frac{L(\mathbf{Y}|f_{\mathbf{X}})}{L(\mathbf{Y})} d\mathbf{Y} \\ &= \mathbb{E}_{p(f_{\mathbf{X}}|\mathcal{D})} [D_{\text{KL}}[L(\mathbf{Y}|f_{\mathbf{X}}) \parallel L(\mathbf{Y})]] \\ &= I(f_{\mathbf{X}}; \mathbf{Y} | \mathcal{D}). \end{aligned} \tag{8}$$

\square

D. Experimental Details

This appendix provides a comprehensive overview of the simulation environment, model parameters, and hyper-parameter choices used to generate the results in this paper. The experiments were designed to be reproducible given the configurations outlined below.

D.1. Simulation Environment

All simulations for the perception failure evaluation in CARLA (Section D.3) were conducted on a Linux workstation with Ubuntu 22.04 LTS equipped with an Intel 13th Gen Core i7-13700KF CPU (16 cores, 24 threads, up to 5.4 GHz) and an NVIDIA GeForce RTX 4090 GPU (24 GB VRAM). The system ran CARLA simulations using CUDA 12.2 and NVIDIA driver version 535.230.02.

All other experiments were run on a MacBook Pro equipped with an Apple M2 Pro processor (10-core CPU, 16-core GPU) and a 3024×1964 Retina display. The GPU supports Metal 3, and the system was used as-is without external accelerators.

All experiments were conducted using Python 3.9. The core scientific computing libraries utilized were:

- BoTorch (Balandat et al., 2020)
- GPyTorch (Gardner et al., 2018)

In all experiments, we utilized the built-in Monte Carlo sampler in Botorch for the optimization of acquisition functions. The Monte Carlo samples are drawn from the posteriors for each model to approximate the expectations of acquisition functions.

D.2. Constrained System Identification

D.2.1. PLUME FIELD MODEL AND PARAMETERS

We consider the monitoring of a chemical plume field, where multiple plume sources generate plume particles that can be measured by sensors. The field function is represented by the rate of hits, defined as the average number of particles per unit time measured by the sensor at a certain location.

The rate of hits for a chemical plume source is given as:

$$R_\theta(x) = \frac{R_s}{\log \frac{\gamma}{a}} \exp\left(-\frac{\langle \theta - x, V \rangle}{2D}\right) K_0\left(\frac{\|\theta - x\|_2}{\gamma}\right),$$

where θ is the location of the plume source, R_s is the rate at which the plume source releases the plume particles in the environment, $\gamma = \sqrt{D\tau/(1 + \frac{\|V\|^2\tau}{4D})}$ is the average distance traveled by a plume particle in its lifetime, a is the size of the sensor detecting plume particles, V is the average wind velocity, D is the diffusivity of the plume particles, and K_0 is the Bessel function of zeroth order.

The measurement y , *i.e.*, the number of particles measured, is modeled as a Poisson random variable with $R_\theta(x)\Delta t$ as the rate parameter, which leads to a likelihood model as

$$L_\theta(y|x) = \frac{\exp(-R_\theta(x)\Delta t)(R_\theta(x)\Delta t)^y}{y!},$$

where Δt is the time taken to obtain a measurement.

General Field and Sensor Parameters:

- Grid Size: 100×100 units.
- Sensor Size (a): 1.0 units.
- Measurement Time (Δt): 1.0 seconds.

Source Parameters: Eight potential plume sources were defined for the experiments. Their specific physical parameters are detailed as:

SOURCE	θ	R_s	γ	V	D
1	[20.0, 20.0]	100.0	50.0	[0.5, 0.5]	10
2	[30.0, 80.0]	100.0	60.0	[-0.3, 0.2]	15
3	[45.0, 55.0]	15.0	50.0	[0.5, 0.5]	10
4	[50.0, 50.0]	18.0	30.0	[-0.3, 0.2]	15
5	[55.0, 45.0]	16.0	40.0	[0.2, -0.4]	12
6	[48.0, 52.0]	17.0	35.0	[0.1, 0.1]	11
7	[52.0, 55.0]	14.0	45.0	[-0.1, -0.1]	13
8	[52.0, 52.0]	18.0	40.0	[0.1, -0.1]	13

D.2.2. TASK-SPECIFIC CONFIGURATIONS

Source Localization.

- Goal: Estimate the unknown location $\theta = [x, y]$ of a single active source.
- Ground Truth: Source 1 was configured as the single active source.
- Maximum Sensor Threshold (y_{max}): 60.0 hits/second.
- Hypothesis Space: A discrete grid of potential locations spanning $[0,100] \times [0,100]$ with a resolution of 5 units, resulting in a 20×20 grid of 400 hypotheses.
- Degree of curiosity: $\beta = 0.5$.

Wind Estimation.

- Goal: Estimate the unknown wind vector $V = [v_x, v_y]$ for a single source with a known location.
- Ground Truth: Source 2 was used, with its true wind vector set to [-0.3, 0.2].
- Maximum Sensor Threshold (y_{max}): 60.0 hits/second.
- Hypothesis Space: A discrete grid of potential wind vectors spanning $[-1,1] \times [-1,1]$ with a resolution of 0.1 units, resulting in a 20×20 grid of 400 hypotheses.
- Degree of curiosity: $\beta = 1.0$.

Active Source Identification.

- Goal: Identify the subset of active sources from a set of six potential sources with known locations.
- Ground Truth: Sources 3-8 were used, with Sources 3, 5, 6, and 8 were set as active.
- Maximum Sensor Threshold (y_{max}): 30.0 hits/second.
- Hypothesis Space: The set of all possible on/off combinations for the six sources. This is a discrete space with $2^6 = 64$ unique hypotheses.
- Degree of curiosity: $\beta = 5.0$.

D.3. Constrained Active Search

D.3.1. PERCEPTION IN SELF DRIVING SIMULATION CARLA

We consider the failure discovery for YOLO-based object detection (Jiang et al., 2022; Redmon & Farhadi, 2018) in the CARLA simulator (Dosovitskiy et al., 2017).

This requires the generation of various scenarios in the environment using CARLA simulator. The environment is a composition of a static context and scenario ϕ . We use the probabilistic programming framework Scenic (Fremont et al.,

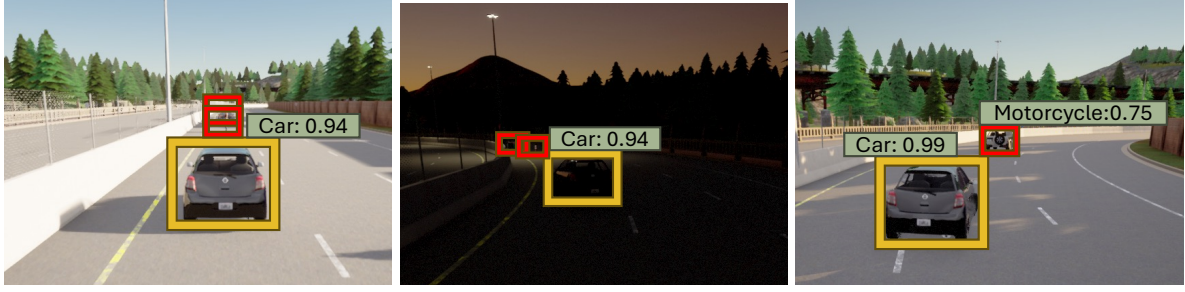


Figure 4. Examples of missed object detection by YOLO due to two reasons considered in perception failure case study in Section D.3. Fig (left to right): example of Failure-1 (distance), Failure-2 (poor light) and Failure-1 and Failure-2 both in one scene (distance and poor light), respectively. Bounding boxes for detected objects (misdetections) shown in yellow (red) with detection confidence numbers. Each scene has two cars and a pedestrian.

2019) for sampling scenarios with varying contextual information for a fixed scenario variable ϕ . For the simulations presented in this paper, we used a publically available, pre-existing environment (Dreossi et al., 2019), which consists of the ego vehicle maneuvering on the road with two non-ego agents—two non-ego cars and a pedestrian crossing the road. We use YOLO object detection model to detect all non-ego agents in a scene. The generated scenario is seeded for reproducibility, so that for a given scenario ϕ , the environment can be treated as a deterministic quantity. Each scenario is defined using $\phi = [b_e, b_l, s]$, where $b_e, b_l \in [5, 15]$ represent the braking threshold of the ego car and lead car (non-ego car in-front of ego car) (m) and $s \in [0, \pi/2]$ denotes the sun altitude angle (rad). Each of these quantities is normalized to be within $[0, 1]$, and the normalized scenario is chosen as the decision variable x for active inference.

We are interested in environment variables (scenarios) that lead to two specific types of failures—failure to detect non-ego agents due to large distance from ego vehicle (Failure 1), and failure to detect non-ego agents due to poor scene lighting (Failure 2). Fig. 4 shows examples of the discussed object detection failures we aim to discover.

D.3.2. LLM-BASED EVALUATION FOR CARLA

We use LLM to perform evaluations for whether a generated scene corresponds to a failure due to specific type.

Each evaluation for a specific scenario corresponds to $T = 60$ steps of simulations. Images recorded from the camera view are used for object detection and classification at every 10 steps using YOLO-v3 (Redmon & Farhadi, 2018), and the classified image are used as inputs to GiT (Wang et al., 2022) to predict a likely failure type based on fine-tuning data.

Results obtained from YOLO along-with the reports from GiT are used as inputs to GPT3 model for failure evaluation, which is queried 6 times per evaluation, and assigns binary scores pertaining to each failure mode for each scene (camera image). The average value reported across 6 scenes is used to construct $c_i : \mathcal{Z} \rightarrow \mathbb{R}$ for $i = 1, 2$ as: $c_i(z) = \frac{1}{T} \sum_{t=1}^T b_t^i$. Here $b_t^i \in \{0, 1\}$ is a scene-specific binary evaluation provided by the LLM based on report generated by GiT to assess if an object detection failure is observed in a given scene and corresponds to Failure- i .

We use GPT-3.5 Turbo model for LLM-based binary evaluations, with each evaluation we query the LLM 6 times and combine the binary evaluations for all 6 runs. Note that usage of LLM is not a core part of our methodology and is only used to as a subjective evaluator.

We show the prompt used for failure evaluation of each scene using the LLM in the box below. Information shown in **red** and **blue** is obtained from GiT captioning system, and CARLA respectively. The output of the LLM is used to obtain a binary number for each scene which is composed to give a scenario specific cost function c_1, c_2 .

D.3.3. TASK-SPECIFIC CONFIGURATIONS

- Goal: We consider two cost functions c_1, c_2 associated with each type of failure. The goal is to sample from the set $\Omega = \{z | c_1(z) \geq C_1, c_2(z) \geq C_2\}$, and we consider three target sets defined by $C_1 = C_2 = 0.1$, $C_1 = C_2 = 0.5$, and $C_1 = C_2 = 0.8$.
- Degree of curiosity: $\beta = 20.0$.

Prompt Used for CARLA evaluation

You will be provided the analysis of YOLO Object detection on an image that was taken from the camera feed of CARLA simulator. The simulator is simulating a pedestrian crossing the road before a car in front of the ego car. There are two cars and one pedestrian in each image.

The information provided:

1. *Objects detected*: List of objects detected by YOLO in the image. This list should have atleast one object from the *Objects to detect* list
2. *Objects to detect* list:
 - One object with one of the following labels: 'car', 'truck',
 - One object with one of the following labels: 'car', 'truck', 'bus', 'motorcycle', 'bicycle'
 - One object with one of the following labels: 'person'
3. Reason: The reason is a brief explanation of the failure to detect all objects, if that happens, and is generated by a pre-trained GiT model in the form of captions for the image.

We are looking to discover images where YOLO fails to detect an object due to **bad light** and/or **large distance**. If the list of *objects detected* has an object missing from the *objects to detect* list, look at the reason. The reason can have other components as well, but it can 'only' be considered as **bad light** if at least one of the objects was failed to detect strictly due to **bad light**. Similarly, the reason can have other components as well, but it can 'only' be considered as **large distance** if the reason contains the phrase 'far away'. Follow the response instructions while responding.

Response Instructions: Respond should be an integer 0, 1, 2, 3 or 4:

- 0 indicating that at least one object was missing from the 'objects to detect' list, but the reason provided does not correspond to bad light or large distance.
- 1 indicating that an object was not detected and the reason provided corresponds to bad light only.
- 2 indicating that an object was not detected, and the reason corresponds to large distance only.
- 3 indicating that an object was not detected, and the reason corresponds to both large distance and bad light.
- 4 indicating all objects are detected. Do not provide explanation.

Response format: Response: [integer], where integer = 0,1,2,3,4.

The list of objects detected and reason for incomplete detection for the image are as follows:

- Objects detected: {objects}
- Reason: {reason}

D.4. Composite Bayesian Optimization

D.4.1. PREFERENCE EVALUATION

We simulate human-in-the-loop or policy-driven decision-making via pairwise preference queries. That is, for selected pairs of outcomes (y_1, y_2), a preference function indicates which design is preferred. These preferences are generated based on a latent utility function, not revealed to the optimizer.

An initial set of 1 pairwise preferences is randomly sampled to initialize the model. Each step of the optimization selects new pairs to query, guided by the used acquisition strategy.

D.4.2. TASK-SPECIFIC CONFIGURATIONS

Vehicle Safety.

- Goal: Optimize vehicle crash-worthiness.
- Testbed: See [Tanabe & Ishibuchi \(2020\)](#) for details.
- Ground Truth Preference: $g(y) = -(y - y^*)^2$, where $y^* = [1864.7202, 11.8199, 0.2904]$.
- Degree of curiosity: $\beta = \gamma = 1.0$.

Penicillin.

- Goal: Maximize the penicillin yield while minimizing time to ferment and the CO2 byproduct.
- Testbed: See [Liang & Lai \(2021\)](#) for details.
- Ground Truth Preference: $g(y) = -(y - y^*)^2$, where $y^* = [25.935, 57.612, 935.5]$.
- Degree of curiosity: $\beta = \gamma = 1.0$.

Energy Resource Allocation.

- Goal: Identify deployment strategies for Distributed Energy Resources (DERs) in Optimal Power Flow (OPF) that align with implicit ethical preferences across multiple performance dimensions detailed in the following table.
- Testbed: IEEE 30-bus network in pandapower library.
- Ground Truth Preference: $g(y) = a^\top y$, where $a = [1, -1, 2, 1]$
- Degree of curiosity: $\beta = \gamma = 1.0$.

Performance Metrics	Definition
Voltage Fairness	Measures the variance in bus voltages across the network; lower variance implies more equitable voltage delivery.
Total Cost	Combines capital expenditures for DER installation and operational costs related to reactive power support.
Priority Area Coverage	Quantifies the share of power delivered to high-priority buses, such as rural or underserved regions.
Resilience	Assesses the percentage of time that all bus voltages remain within safe operating limits under perturbations (e.g., load uncertainty or line outages).

D.4.3. EXTENDED BASELINE COMPARISON WITH BOPE

To highlight the benefits of jointly learning and optimizing, rather than separating these into stages, we extend the baseline comparison with **BOPE** from [Lin et al. \(2022\)](#).

The original BOPE framework is intentionally flexible and leaves many problem-specific design choices open, especially regarding how and when to switch between preference exploration and experimentation. In our comparison, we consider four representative stage-wise variants:

- **BOPE-I:** A two-phase strategy that starts with qEUBO (preference-focused exploration) and switches to qNEI in the second half (objective-driven refinement), illustrating the effect of premature exploitation.
- **BOPE-II:** A two-phase strategy that starts with qNEI (exploring the objective space) and switches to qEUBO in the second half (exploiting the learned preference model), using a frozen outcome snapshot for qEUBO.
- **BOPE-III:** A qEUBO-only variant where experiments are selected by qEUBO with a newly sampled objective realization at each iteration, encouraging stronger exploration through objective variation.

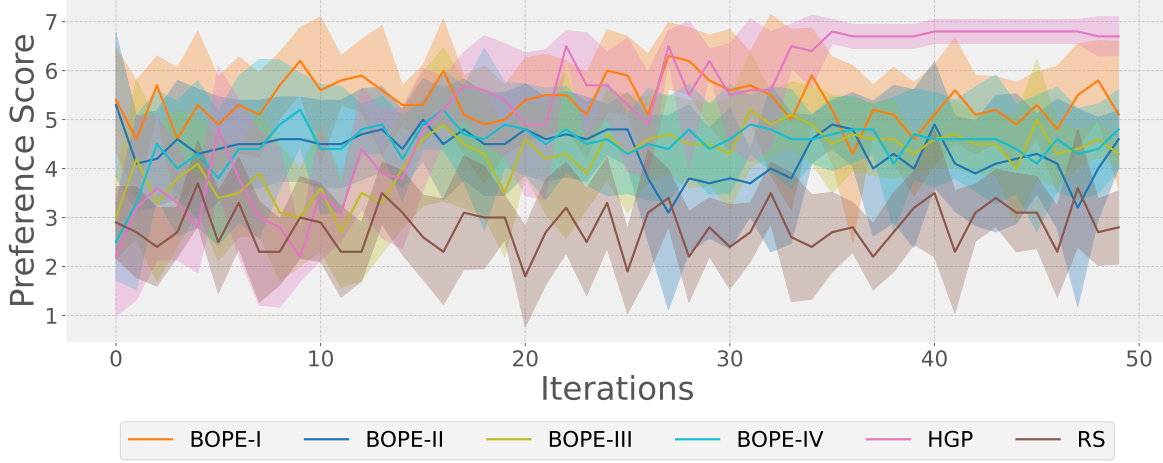


Figure 5. Extended baseline comparison with BOPE for energy resource allocation. Error bars represent ± 1 standard deviation over 5 seeds.

- **BOPE-IV:** A BOPE variant that uses standard preference exploration (qEUBO) and selects experiments exclusively with qNEI, fully refitting both outcome and preference GPs after each update.

Figure 5 reports their preference scores over random sampling (**RS**). It is evident that our active-inference method for hierarchical GPs (**HGP**) consistently discovers higher-preference regions after a brief initial exploration phase, while BOPE variants are highly sensitive to their stage-wise design choices. **BOPE-I**, being preference-driven in the first phase, initially attains higher preference values but fails to balance exploration and exploitation, leading to poor convergence in the second half; its performance is also sensitive to the precise switching point. **BOPE-II** explores first and then optimizes, achieving better final performance than BOPE-I, but the strict separation between exploration and exploitation still yields suboptimal outcomes. **BOPE-III** mixes both aspects but remains more exploitation-centric, performing better than BOPE-I/II yet still below HGP. **BOPE-IV** and HGP share the idea of refitting both models at each step, but BOPE-IV converges to a lower-preference solution. In contrast, our acquisition strategy jointly leverages information from both the outcome and preference models at every iteration, leading to higher sample efficiency and more reliable discovery of high-preference regions.

E. Use of Large Language Models

We use LLM to revise and polish drafts of the introduction, abstract, conclusion, and limitations sections to enhance clarity, flow, and accessibility for a broader audience.

We also use LLM as an evaluator for the experiments of failure discovery in CARLA, which is detailed in Appendix D.3.